Experiment on Impedance Adaptation for an Under-Actuated Gripper Grasping an Unknown Object with Tactile Sensing

Shaobo Yan[1(✉)], Zhongyi Chu[1], and Fuchun Sun[2]

[1] School of Instrument Science and Opto-Electronics Engineering, Beihang University, Beijing 100191, China
yan7shark@126.com
[2] Department of Computer Science and Technology, Tsinghua University, Beijing, China

Abstract. This paper presents an experiment on impedance adaptation for an under-actuated gripper grasping an unknown object. Under-actuated gripper has broad applications in the field of industrial robotics and on-orbit services because of its better self-adaption. However, subject to uncertain characteristics of the object, it is difficult for an under-actuated gripper to achieve stable grasp. To address this problem, this paper develops impedance adaptation for an under-actuated gripper manipulation with the tactile sensing. A cost function that measures the contact force, velocity and positioning errors of the contact point is defined and the critical impedance parameters are determined that minimize it; this adaptation is feasible for an under-actuated gripper to guarantee a stable grasp without requiring information on the object dynamics. Finally, an experimental setup is established to verify the validity of the proposed method. The experimental results demonstrate that the under-actuated gripper can stably grasp an unknown object.

Keywords: Stable grasp · Impedance adaptation · Under-actuated gripper · Tactile sensing · Unknown object

1 Introduction

In the fields of industrial robotics and on-orbit services, end effectors play an important role. As a type of end effector, an under-actuated gripper [1] has a broad range of applications because of its better self-adaption abilities, which permit the grasp of objects of various shapes. Due to the under-actuated characteristics, many different types of passive elements, such as springs, are considered to resolve the non-uniqueness question involved with null space grasping and ensuring the shape-adaptation of the finger to the object grasped [2]. It is worth mentioning that the balance between the contact force, the input torque and the spring passive torque contribute to various grasping types and has a significant effect on stable grasping. A proper contact force is necessary for stable grasp. Commonly, the contact force applied is either too weak or too strong, resulting in slipping or mechanical deformation of the grasped object [3]. Generally, the necessary contact force is different for the

F. Sun et al. (Eds.): ICCSIP 2016, CCIS 710, pp. 247–260, 2017.
DOI: 10.1007/978-981-10-5230-9_27

objects with different parameters. However, the contact force is a passive parameter one cannot directly control. Considering the balance between the contact force, the spring torque and the input torque, the contact force can be adjusted by controlling the input torque. Hence, it is essential to control the input torque depending on the properties of the object.

In this field, impedance control [4] can be employed to achieve a stable grasp [5]. Under impedance control, an under-actuated gripper's compliance is determined by contact force exerted by the object. Moreover, impedance control regulates the contact force implicitly by specifying the desired impedance [6]. In early research works on impedance control, the uncertainties in robotic dynamics are considered in order to obtain the desired impedance model [7]. However, in many situations, the environmental dynamics should be taken into account. A good control strategy is to choose the proper impedance parameters based on the object. As a result, impedance adaptation has been widely investigated. In [8], an impact controller based on the switching of the impedance parameters depending on dissipated and generated forms of energy is discussed. In [9], the position data and contact force are used to obtain the desired impedance parameters based on adaptive optimal control. In many studies on impedance control, the environmental parameters are estimated to design the impedance controller. For example, the stiffness of a human operator's arm is estimated in real-time based on which controller is designed to adjust the impedance coefficients of the robot [10].

For impedance adaptation, optimization is necessary because that the control objective of impedance control includes both force regulation and trajectory tracking. In [11], a cost function measuring trajectory errors and contact force is defined. The desired impedance parameters are obtained to minimize the cost function. However, the system dynamics are assumed to be known. To achieve optimal control in the case of unknown system dynamics, adaptive dynamic programming (ADP) has been widely studied [12]. In many studies of ADP, a learning process is still required to obtain the desired impedance parameters, which causes the robot to repeat operations to learn the desired impedance parameters [13]. In [9], this problem is avoided by modifying the ADP for systems with unknown dynamics. Although impedance adaptation has been broadly developed it is challenging to employ it to solve the stable grasp problem because the parameters of the object are unknown. This is especially for an under-actuated gripper. It is difficult to develop impedance adaptation because it is impossible to control the position of each phalanx independently.

In our previous works, an under-actuated gripper was designed and manufactured. The under-actuated gripper consists of two under-actuated fingers with a rotational spring which is placed in a different location from that of the SARAH hand to resolve the indeterminacy so that the distal phalanges can move relative to one another in a parallel manner with less energy consumption [14]. Moreover, an impedance joint torque controller has been designed to control the grasping system dynamics [15]. However, the parameters of the controller are treated as a constant, and a controller with fixed parameters does not suffice in many applications. For example, the parameters of the grasped object are usually unknown. To achieve stable grasp with an unknown object, this paper develops an impedance adaptation on a two-finger under-actuated gripper using tactile sensing. First, a terrestrial experimental setup is

established using the two-finger under-actuated gripper, an unknown grasped object and hardware control architecture. Second, the object dynamics are taken into consideration to develop the impedance adaptation, and the unknown grasped object is described as a mass-damping-stiffness system with unknown dynamics. Then, the desired impedance model is obtained based on the unknown dynamics, and the critical impedance parameters are determined that minimize the cost function which is defined to describe the grasp performance. Furthermore, an impedance model is imposed on the under-actuated gripper to guarantee a stable grasp. Finally, the experimental results are used to validate the stability and adaptability of the design at grasping an unknown object.

The remainder of this paper is organized as follows. In Sect. 2, the mechanism and experimental setup are described. In Sect. 3, the impedance adaptation is developed based on an estimation of the parameters of the unknown object and optimal control so that the stable grasping is achieved based on the unknown object. In Sect. 4, the validity of the proposed method is verified through experimentation. Section 5 concludes the paper.

2 Mechanism and Experimental Setup

As shown in Fig. 1, the experimental system consists of two parts: a supervisor computer and an implementation controller. Based on the SCI (Serial Communication Interface) software, the supervisor computer displays the measurements. The implementation controller consists of a 2-finger under-actuated gripper, the unknown grasped object and the hardware control architecture, which comprise a closed-loop control system.

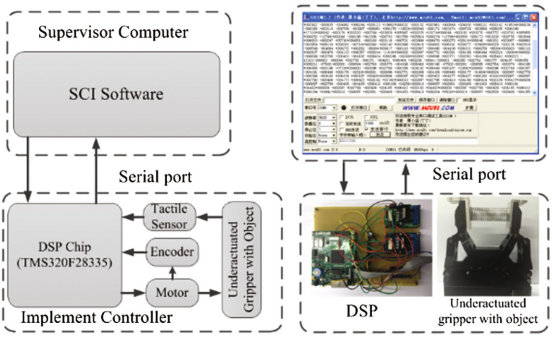

Fig. 1. The experimental system.

2.1 Mechanism

The model of the under-actuated gripper and unknown grasped object is shown in Fig. 2. The under-actuated gripper consists of four parts: the driving and transmission portion, the gripper portion, the tactile sensor and the support portion, as shown in

Fig. 3. The driving and transmission portion consists of one driving motor, two gear wheels, two worm gears and two worm screws. The gripper portion consists of two under-actuated fingers with rotational springs, i.e., passive actuators. Each under-actuated finger is a closed-loop system with five linkages, the driving linkage, the driven linkage, the middle linkage, the contact linkage and the linkage embedded in the base. The spring is located between the driving and middle linkages. Most importantly, a PPS (Pressure Profile System) tactile sensor SN5570 is fixed on the contact linkage used to measure the contact force. The support portion is the base that supports the entire system. The parameters of the under-actuated gripper are listed in Table 1.

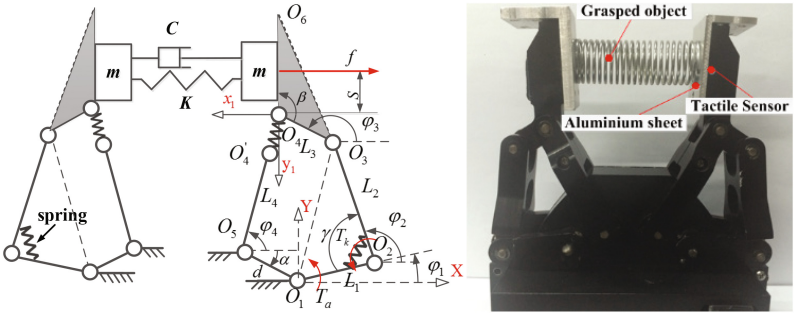

Fig. 2. The under-actuated gripper with an unknown grasped object.

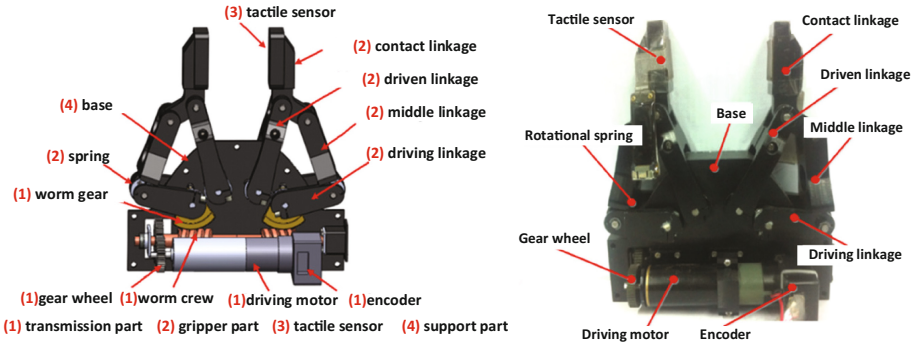

Fig. 3. The structure of the under-actuated gripper.

Table 1. The parameters of the gripper.

Symbol	Value	Symbol	Value
L_1	3.18×10^{-2} m	d	1.90×10^{-2} m
L_2	4.80×10^{-2} m	α	0.46 rad
L_3	1.90×10^{-2} m	β	2.09 rad
L_4	5.71×10^{-2} m		

In this paper, the grasped objects are chosen to be three sets of springs with different stiffnesses, as shown in Fig. 4. An aluminium sheet (shown in Fig. 2) is placed between the grasped spring and the PPS tactile sensor to ensure that the spring contact with the PPS sensor is over a large area.

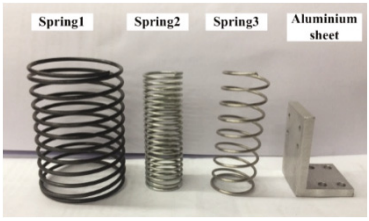

Fig. 4. Springs and aluminium sheet

2.2 Hardware Control Architecture

As illustrated in Fig. 1, the proposed hardware control architecture consists of a multisensory system, a controller and communication system. The multisensory system consists of motor and sensors. The under-actuated gripper is driven by a Maxon motor and a worm gear (gear ratio 1:35). A photoelectric encoder (HEDS 5X40) with a 500 pulse/rev capability is embedded in the motor to provide rotor position/speed. An integrated circuit converts the two-phase input pulses into a four-phase-count, which improves the precision of measurement. From on this data, the positional data of contact point is obtained based on the kinematic of the under-actuated gripper. Additionally, the PPS sensor on the contact linkage provides the contact force data, which consists of 4×4 sensing cells and signal processing circuitry. This array of sensors ensures the accuracy of the measurement, and the signal processing circuitry is used to transmit of the measured data.

For the under-actuated gripper and unknown grasped object, the controller is integrated onto a DSP chip (TMS320F28335), which is used to perform sensor signal processing and motor control, as well as communicating between the under-actuated gripper and the PC. The position and contact force data are sent to the DSP to ensure closed-loop control. Combined with the control algorithm, several PWM pulses with the proper duty ratio are output from the DSP depending on the particular motor being driven by the driving circuit (L298N) to grasp an unknown grasped object.

3 Impedance Adaptive Control

This section is dedicated to develop impedance adaptive control. The proposed impedance adaptive control scheme of the system is shown in Fig. 5. A desired impedance model is imposed on the under-actuated gripper to ensure stable grasping, and the impedance parameters determined from an unknown grasped object are based on the estimation of the object's parameters. In particular, the desired impedance model is given by

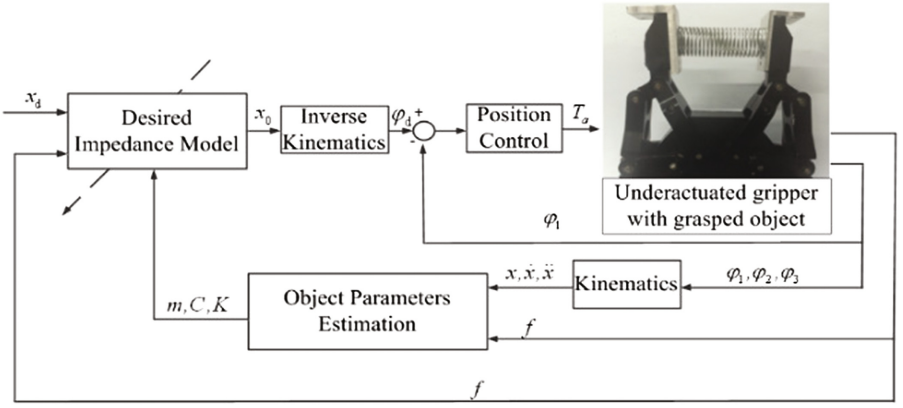

Fig. 5. Schematic of the impedance adaptive control.

$$f = \mathrm{Z}(x_0, x_d), \tag{1}$$

where x_d is the desired trajectory of the contact point, x_0 is the virtual desired trajectory and Z(·) is a target impedance function that needs to be determined. For an ideal position controller, it is obvious that $x_0(t) = x(t)$. Then, the desired impedance model can be rewritten as

$$f = \mathrm{Z}(x, x_d). \tag{2}$$

The method to determine Z(·) is presented in the following subsections. It is worth mentioning that the desired impedance model is based on the unknown grasped object. Therefore, the unknown grasped object is analysed to develop the impedance adaptive control, and the description of the unknown grasped object is presented in Sect. 3.1.

3.1 Description of the Unknown Grasped Object

As shown in Fig. 3, and without the loss of generality, the unknown grasped object is described as mass-damping-stiffness system. The dynamic equation for the unknown grasped object is given by:

$$f = -m\ddot{x} - 2C\dot{x} - 2Kx, \tag{3}$$

where m, C and K are the unknown contact mass, damping and stiffness of the grasped object model, respectively. The variable f denotes the force exerted by the contact linkage. The variables $\ddot{x}$, $\dot{x}$ and x are the acceleration, velocity and position of the contact point, respectively, which change along the x_1 axis. For a mass-damping-stiffness system, the state function is defined as:

$$\dot{\boldsymbol{\xi}} = \mathbf{A}\boldsymbol{\xi} + \mathbf{B}\mathbf{u}, \tag{4}$$

where $\boldsymbol{\xi}$ is the system state, $\mathbf{u}$ is the system input, and $\mathbf{A}$ and $\mathbf{B}$ are unknown constant matrices related to the parameters of grasped object (m, C and K). In this paper, the system input is $\mathbf{u} = [f]$, and the system state is $\boldsymbol{\xi} = [\dot{x} \quad x \quad \mathbf{z}]^{\mathrm{T}}$, in which $\mathbf{z} \in \mathbf{R}^m$ is the state of the following system [11]:

$$\begin{cases} \dot{\mathbf{z}} = \mathbf{U}\mathbf{z}, \\ x_d = \mathbf{V}\mathbf{z}, \end{cases} \tag{5}$$

Where $\mathbf{U} \in \mathbf{R}^{m\times m}$ and $\mathbf{V} \in \mathbf{R}^{n\times m}$ are two known matrices. Substituting Eq. (3) into Eq. (4), the state function can be rewritten as:

$$\begin{bmatrix} \ddot{x} \\ \dot{x} \\ \dot{\mathbf{z}} \end{bmatrix} = \begin{bmatrix} -2\mathrm{C}m^{-1} & -2Km^{-1} & \mathbf{0} \\ \mathbf{I} & \mathbf{0} & \mathbf{0} \\ \mathbf{0} & \mathbf{0} & \mathbf{U} \end{bmatrix} \begin{bmatrix} \dot{x} \\ x \\ \mathbf{z} \end{bmatrix} + \begin{bmatrix} -m^{-1} \\ \mathbf{0} \\ \mathbf{0} \end{bmatrix} f. \tag{6}$$

We denote

$$\mathbf{A} = \begin{bmatrix} -2\mathrm{C}m^{-1} & -2Km^{-1} & \mathbf{0} \\ \mathbf{I} & \mathbf{0} & \mathbf{0} \\ \mathbf{0} & \mathbf{0} & \mathbf{U} \end{bmatrix}, \mathbf{B} = \begin{bmatrix} -m^{-1} \\ \mathbf{0} \\ \mathbf{0} \end{bmatrix}. \tag{7}$$

Note that $\mathbf{A}$ and $\mathbf{B}$ include the grasped object dynamics and that they are unknown.

3.2 Impedance Adaptation

By addressing the grasped object dynamics, we develop an impedance adaptation to minimize the following cost function:

$$\begin{aligned} \boldsymbol{\Gamma} &= \int_0^\infty (\dot{x}^{\mathrm{T}} Q_1 \dot{x} + (x - x_d)^{\mathrm{T}} Q_2 (x - x_d) + f^{\mathrm{T}} r f) dt \\ &= \int_0^\infty (\dot{x}^{\mathrm{T}} Q_1 \dot{x} + \begin{bmatrix} x^{\mathrm{T}} & \mathbf{z}^{\mathrm{T}} \end{bmatrix} \begin{bmatrix} Q_2' & -Q_2' V \\ -V^{\mathrm{T}} Q_2' & V^{\mathrm{T}} Q_2' V \end{bmatrix} \begin{bmatrix} x \\ \mathbf{z} \end{bmatrix} + f^{\mathrm{T}} r f) dt \\ &= \int_0^\infty [\boldsymbol{\xi}^{\mathrm{T}} \mathbf{Q} \boldsymbol{\xi} + f^{\mathrm{T}} \mathbf{R} f] dt. \end{aligned} \tag{8}$$

The cost function presented in Eq. (8) represents the compromise/combination of the force regulation and trajectory tracking and determines the grasping performance. In Eq. (8), $\mathbf{Q}$ and $\mathbf{R}$ are the weighting matrices which satisfy:

$$\mathbf{Q} = \mathbf{Q}^{\mathrm{T}} = \begin{bmatrix} Q_1 & \mathbf{0} & \mathbf{0} \\ \mathbf{0} & Q_2' & -Q_2'\mathbf{V} \\ \mathbf{0} & -\mathbf{V}^{\mathrm{T}} Q_2' & \mathbf{V}^{\mathrm{T}} Q_2' \mathbf{V} \end{bmatrix}, \mathbf{R} = [r]. \tag{9}$$

The factors Q_1 and $Q_2^{'}$ satisfy: $Q_1 > 0$, $Q_2^{'} > 0$, and $r > 0$. If we assume the contact force f in Eq. (6) to be the 'system input' to the grasped object dynamics, we are able to obtain a minimized version of the cost function (Eq. 8). The optimal control state is then can be employed to determine the contact force f, which is obtained as follow

$$f = -\mathbf{K}_k \boldsymbol{\xi} = -\mathbf{R}^{-1} \mathrm{B}^{\mathrm{T}} \mathbf{P} \boldsymbol{\xi}, \tag{10}$$

where $\mathbf{K}_k$ is the optimal feedback gain matrix and $\mathbf{P} = \mathbf{P}^{\mathbf{T}}$ is the solution of the following Riccati equation

$$\mathbf{PA} + \mathbf{A}^{\mathrm{T}}\mathbf{P} - \mathbf{PBR}^{-1}\mathbf{B}^{\mathrm{T}}\mathbf{P} + \mathbf{Q} = \mathbf{0}. \tag{11}$$

We denote that

$$\mathbf{P} = \begin{bmatrix} \mathbf{P}_1 & \mathbf{P_2} & \mathbf{P_3} \\ * & * & * \\ * & * & * \end{bmatrix}, \tag{12}$$

where $\mathbf{P}_1 \in \mathbf{R}^{n \times n}$, $\mathbf{P_2} \in \mathbf{R}^{n \times n}$ and $\mathbf{P_3} \in \mathbf{R}^{n \times n}$, and '*' represents the elements that do not concern this problem. Substituting Eq. (12) into Eq. (10) leads to

$$\begin{aligned} f &= m^{-1}\mathbf{R}^{-1}\mathbf{P_1}\dot{x} + m^{-1}\mathbf{R}^{-1}\mathbf{P_2}x - m^{-1}\mathbf{R}^{-1}\mathbf{P_3}\mathbf{z} \\ &= m^{-1}\mathbf{R}^{-1}[\mathbf{P_1}\dot{x} + \mathbf{P_2}x - \mathbf{P_3}\mathbf{V}^{\mathrm{T}}(\mathbf{V}\mathbf{V}^{\mathrm{T}})^{-1}x_{\mathrm{d}}] \\ &= -k_0\dot{x} - k_1 x - k_2 x_{\mathrm{d}}. \end{aligned} \tag{13}$$

For certain values of $\mathbf{A}$, $\mathbf{B}$, $\mathbf{Q}$ and $\mathbf{R}$, the values of k_0, k_1 and k_2 may be obtained by solving the Riccati equation:

$$k_0 = -\sqrt{Q_1^2/r - 2mk_1 + 4C^2} + 2C, \tag{14}$$

$$k_1 = -\sqrt{Q_2^{'}/r + 4K^2} + 2K, \tag{15}$$

$$k_2 = \mathrm{Q}_2^{'}\mathbf{V}r^{-1}(k_0\mathbf{U} - 2C\mathbf{U} + m\mathbf{U}^2 + 2K\mathbf{I} - k_1\mathbf{I})^{-1}\mathbf{V}^{\mathrm{T}}(\mathbf{V}\mathbf{V}^{\mathrm{T}})^{-1}. \tag{16}$$

For the unknown parameters (m, C and K) of the grasped object, an estimation method is developed based on the Recursive Least Squares (RLS) algorithm. For the detailed implementation, we recall from the Eq. (3) that each $k \in Z^+$, where k stands for step k and Z^+ is positive integer. The discretization of Eq. (3) is defined as:

$$f(k) = -m\ddot{x}(k) - 2C\dot{x}(k) - 2Kx(k). \tag{17}$$

Equation (17) can be rewritten as matrix form as:

$$\mathbf{f}(k) = -\mathbf{r}^{\mathrm{T}}(k)\mathbf{w}, \tag{18}$$

where

$$\mathbf{r}(k) = [\ddot{x}(k) \quad 2\dot{x}(k) \quad 2x(k)]^{\mathrm{T}}, \tag{19}$$

$$\mathbf{w} = [m \quad C \quad K]^{\mathrm{T}}. \tag{20}$$

The RLS estimation of $\mathbf{w}$ from [15] is defined as:

$$\hat{\mathbf{w}}(t) = \hat{\mathbf{w}}(t-1) + \mathbf{L}(t)[\mathbf{f}(t) - \mathbf{r}^{\mathrm{T}}(t)\hat{\mathbf{w}}(t-1)], \tag{21}$$

where

$$\mathbf{L}(t) = \mathbf{P}(t-1)\mathbf{r}(t)[1 + \mathbf{r}^{\mathrm{T}}(t)\mathbf{P}(t-1)\mathbf{r}(t)]^{-1}, \tag{22}$$

$$\mathbf{P}(t) = [\mathbf{I}_3 - \mathbf{L}(t)\mathbf{r}^{\mathrm{T}}(t)]\mathbf{P}(t-1). \tag{23}$$

The variable $\mathbf{P}(t)$ is the covariance matrix for a matrix size of 3×3, and $\mathbf{P}(0) = \mathrm{p}_0\mathbf{I}_3$, where p_0 is a large positive number, e.g., $\mathrm{p}_0 = 10^6$. We defining the estimation error as $\delta = \hat{w}(t) - \mathrm{w}$, which approaches zero when the input signal is persistently excited, and when the noise has a zero mean and finite variance [16]. Thus, the parameters of grasped object are obtained using the RLS algorithm.

Comparing Eq. (13) with the desired impedance model (Eq. (2)), the exact impedance parameters are obtained. As shown in Fig. 6, the object parameter estimation is for developing the preliminary impedance adaptation, which requires the contact force and the position data of the contact point. The contact force f is measured by tactile sensing with the PPS sensor, and the position data x is calculated according to the geometric relationship between the joint space and work space (as shown in Fig. 6),

$$x = \|\mathbf{D}\|_2 \cdot \cos(\varphi_3 - \varphi_{30}), \tag{24}$$

where

$$\begin{aligned}\mathbf{D} = \begin{bmatrix} d_x \\ d_y \end{bmatrix} - \begin{bmatrix} d_{x0} \\ d_{y0} \end{bmatrix} &= \begin{bmatrix} \cos\varphi_1 & \cos\varphi_2 & \cos\varphi_3 & \cos(\beta+\varphi_3-\pi) \\ \sin\varphi_1 & \sin\varphi_2 & \sin\varphi_3 & \sin(\beta+\varphi_3-\pi) \end{bmatrix} \begin{bmatrix} L_1 \\ L_2 \\ L_3 \\ S \end{bmatrix} \\ &- \begin{bmatrix} \cos\varphi_{10} & \cos\varphi_{20} & \cos\varphi_{30} & \cos(\beta+\varphi_{30}-\pi) \\ \sin\varphi_{10} & \sin\varphi_{20} & \sin\varphi_{30} & \sin(\beta+\varphi_{30}-\pi) \end{bmatrix} \begin{bmatrix} L_1 \\ L_2 \\ L_3 \\ S_0 \end{bmatrix},\end{aligned} \tag{25}$$

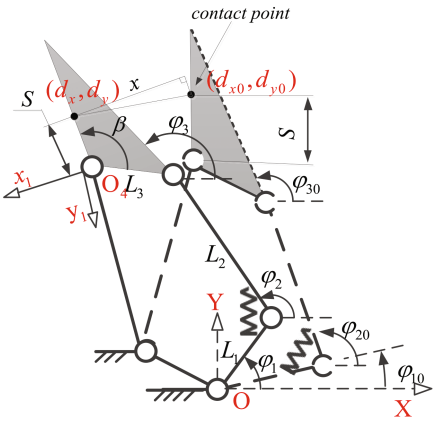

Fig. 6. Geometric relationship between the joint space and the work space.

where $[d_{x0}, d_{y0}]^{\mathrm{T}}$ is the initial position of the contact point, and $[d_x, d_y]^{\mathrm{T}}$ is the current position. The variable S is the distance from the contact point to the joint O_4, and S_0 is the initial value of S. The variable φ_{i0} (i = 1, 2, 3) is the initial value of the joint angle φ_i (i = 1, 2, 3), the joint angle φ_1 is obtained from the photoelectric encoder and the joint angles φ_2 and φ_3 are obtained by solving the following dynamics function for the under-actuated gripper [19].

$$\mathbf{T} = \mathbf{M}(\varphi)\ddot{\varphi} + \mathbf{C}(\dot{\varphi}, \varphi) + \mathbf{H}(\varphi) + \mathbf{T}_{\mathrm{ext}}, \tag{26}$$

where $\boldsymbol{\varphi} = [\varphi_1\ \varphi_2\ \varphi_3\ \varphi_4]^{\mathrm{T}}$ is the vector matrix of the joint angle, $\mathbf{M}(\boldsymbol{\varphi})$ is the inertia matrix of the gripper, $\mathbf{C}(\dot{\varphi}, \varphi)$ denotes the Coriolis and Centrifugal forces, respectively, $\mathbf{H}(\boldsymbol{\varphi})$ is the elastic forces, $\mathbf{T}$ is the vector of the driving motor torque and $\mathbf{T}_{\mathrm{ext}}$ is the reaction torque imposed by an external force.

In brief, based on the object parameter estimation, the parameters presented in Eq. (13) can be determined according to Eqs. (14)–(16). Thus, the virtual desired trajectory x_0 is obtained according to Eq. (13) using the measured f and the given x_d, and the inner-position controller is used to ensure the trajectory tracking. In this way, impedance adaptive control is achieved and Eq. (13) provides the resulting critical impedance function in the presence of an unknown grasped object.

4 Experiment Results

4.1 Experimental Conditions

The proposed method is verified based on the hardware platform presented in Sect. 2. In the control scheme (as shown in Fig. 6), the position control is used to ensure trajectory tracking in joint space, which is achieved by the PID controller. The parameters of the PID controller are chosen as P = 1, I = 0.1 and D = 0. The weighting matrices are chosen as: $Q_1 = 1$, $Q_2^{'} = 800 \times 800$ and $r = 1$. The matrices $\mathbf{U}$ and $\mathbf{V}$ are

chosen as: $\mathbf{U} = \begin{bmatrix} 0 & -1 \\ 0 & 0.5 \end{bmatrix}$ and $\mathbf{V} = [1 \quad 0.01]$, and the desired trajectory is designed to be $x_d = 0.01 - 0.01e^{-0.5t}$. We employing $f = -\mathbf{K}_0\boldsymbol{\xi} + v$ as the impedance model over the time interval [0 s, 3 s], where $\mathbf{K}_0$ is the initial value of the impedance parameters and v is the exploration noise to satisfy the persistent excitation (PE) condition [9]. In the experiment, $\mathbf{K}_0$ is chosen as $\mathbf{K}_0$ = [−1−1000 1000] and the exploration noise is chosen to be $v = \sum_{w=1}^{10} \frac{3}{w} \sin(wt)$. The impedance model for this time period is $f = \dot{x} + 1000x - 1000x_d + v$. The parameters for the grasped object are estimated during the entire process at the same time that the impedance parameters are calculated according to Eqs. (14)–(16). The impedance parameters are used to update the impedance model over the time interval (3 s, 120 s).

4.2 Experimental Results

The experimental results for the position and contact force are shown in Figs. 7(a) and (b). For the three sets of springs with aluminium sheets, the position and contact force converge to constants, and for different springs, the stable position and contact force are different. To observe the effect of the exploration noise, the results over the time interval (0 s, 30 s) are presented in Figs. 7(c) and (d). During the first 3 s, the under-actuated gripper has a high-frequency movement, which ensures an accurate estimation of the parameters of the grasped object. After 3 s, the desired impedance model is obtained and imposed upon the under-actuated gripper, and the action of the

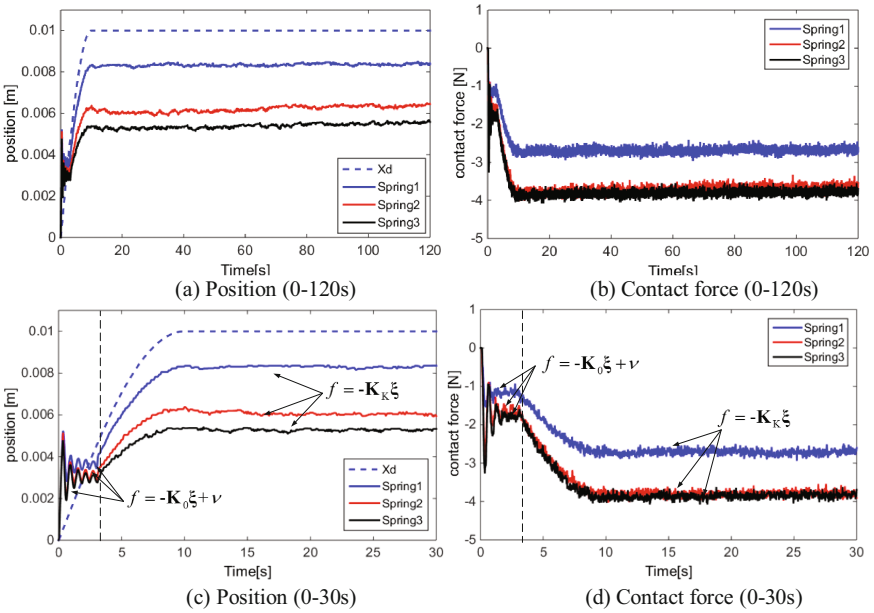

(a) Position (0-120s) (b) Contact force (0-120s)

(c) Position (0-30s) (d) Contact force (0-30s)

Fig. 7. The position and contact force.

under-actuated gripper during this time absolutely relies on the impedance parameters. The convergence performance of the impedance parameters are shown in Fig. 8. For a certain spring with an aluminium sheet, the impedance parameters have a good convergent effect.

For the impedance adaptive control method proposed in Sect. 3, the impedance parameters rely on the estimated values of the dynamics parameters of the springs with an aluminium sheet. The estimated values of the dynamics parameters are presented in Fig. 9, which exhibit good convergent performance.

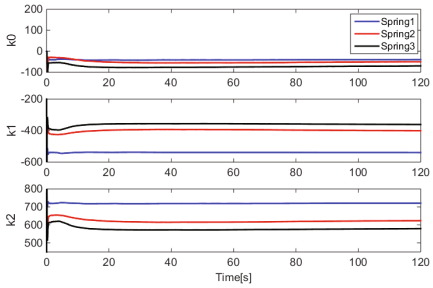

Fig. 8. Impedance parameters.

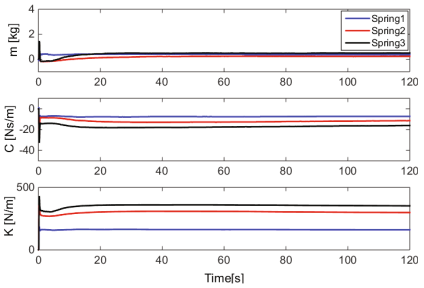

Fig. 9. The estimated values.

The mean values of the estimated results at a stable stage are listed in Table 2, which are compared with the nominal value. The nominal value of the stiffness is measured according to the Hooke's law, and the nominal value of contact mass is given as the mass of the aluminium sheet. However, it is difficult to measure the nominal damping of the spring with an aluminum sheet. From Table 2, we see that the estimation of the stiffness is very near to the nominal value, which has a much larger magnitude than the estimation of the contact mass and damping. Therefore, the stiffness plays a primary role in the grasping process, and an accurate estimation of stiffness is crucial to ensure stable grasping. Although good convergent performance is achieved, there is a significant gap between the nominal mass of the aluminium sheet and the estimation of the contact mass. Additionally, the estimation of the damping is negative and which should be positive in practice. The reason for this result may be that the contact mass and damping of the system composed of the spring and aluminium sheet are much smaller than the stiffness. Thus the estimation of the damping and contact mass is significantly affected by many factors, e.g., measurement error and noise. Despite the fact that a large number of common characteristics are attributed to such a system in which the stiffness is much larger than the contact mass and damping, this work provides a good reference for the stable grasp of an unknown object. Future work should be dedicated to exploring the reason behind the inaccurate estimation of the contact mass and the damping terms. For this work, the selection of a proper grasped object is optional, as well as a viable approach to measuring the damping and contact mass of a grasped object.

Table 2. Estimated results and the nominal value.

	Stiffness (N/m)		Damping (Ns/m)		Contact mass (kg)	
	Nominal value	Estimation	Nominal value	Estimation	Nominal value	Estimation
Spring1	168.9	161.6	DTD	–7.3	0.028	0.37
Spring2	306.3	299.4	DTD	–11.5	0.028	0.22
Spring3	362.9	357.1	DTD	–16.2	0.028	0.49

Note: difficult to determine (DTD).

5 Conclusions

This paper presents an experiment on impedance adaptation for an under-actuated gripper grasping an unknown grasped object with tactile sensing. The experimental setup uses hardware control architecture and a two-finger under-actuated gripper with an unknown grasped object. The unknown grasped objects are chosen as three sets of springs with different stiffness. Based on the hardware platform, an impedance adaptive control is developed to obtain the desired impedance parameters when manipulating an unknown grasped object. The unknown grasped object is described using mass-damping-stiffness system. From this, the desired impedance model is obtained and the critical impedance parameters are determined to minimize a cost function including the velocity, trajectory errors and contact force. The desired impedance model is imposed on the under-actuated gripper to ensure gripper actions during the grasping process. The experimental results show that the under-actuated gripper can stably grasp an unknown grasped object using the proposed method.

Acknowledgements. This work is supported by the Natural Science Foundation of China (Grant Nos. 51375034 and 61327809).

References

1. Kragten, A., van der Helm, F.C.T., Herder, J.L.: A planar geometric design approach for a large grasp range in underactuated hands. Mech. Sci. **46**, 1121–1136 (2011)
2. Birglen, L., Gosselin, C.M.: On the force capability of underactuated fingers. In: Proceedings of IEEE International Conference on Robotics and Automation (2003)
3. Tiwana, M.I., Shashank, A., Redmond, S.J., Lovell, N.H.: Characterization of a capacitive tactile shear sensor for application in robotic and upper limb prostheses. Sens. Actuators A, Phys. **165**(29), 164–172 (2011)
4. Hogan, N.: Impedance control: an approach tomanipulation-part i: theory; part ii: implementation; part iii: applications. Trans. ASME J. Dyn. Syst. Measur. Control **107**, 17–24 (1985)
5. Xu, Q.S.: Robust impedance control of a compliant microgripper for high-speed position/force regulation. IEEE Trans. Ind. Electron. **62**(2), 1201–1209 (2015)
6. Li, M., Hang, K.Y., Kragic, D., Billard, A.: Dexterous grasping under shape uncertainty. Rob. Auton. Syst. **75**(Part B), 352–364 (2016)

7. Colbaugh, R., Seraji, H., Glass, K.: Direct adaptive impedance control of manipulators. J. Rob. Syst. **10**(2), 217–248 (1991)
8. Stanisic, R.Z., Fernandez, A.V.: Adjusting the parameters of the mechanical impedance for velocity, impact and force control. Robotica **30**(4), 583–597 (2012)
9. Ge, S.S., Li, Y.N., Wang, C.: Impedance adaptation for optimal robot–environment interaction. Int. J. Control **87**(2), 249–263 (2013)
10. Tsumugiwa, T., Yokogawa, R., Hara, K.: Variable impedance control based on estimation of human arm stiffness for human-robot cooperative calligraphic task. In: Proceedings of the IEEE International Conference on Robotics and Automation, pp. 644–650 (2002)
11. Johansson, R., Spong, M.W.: Quadratic optimization of impedance control. In: Proceedings of IEEE International Conference of Robotics and Automation, pp. 616–621 (1994)
12. Jiang, Y., Jiang, Z.P.: Computational adaptive optimal control for continuous-time linear systems with completely unknown dynamics. Automatica **48**, 2699–2704 (2012)
13. Kim, B., Park, J., Park, S., Kang, S.: Impedance learning for robotic contact tasks using natural actor-critic algorithm. IEEE Trans. Syst. Man Cybern.-Part B: Cybern. **40**, 433–443 (2010)
14. Chu, Z.Y., Hu, J., Lei, Y.A.: An adaptive gripper of space robot for space on-orbit services, CN 201310326633.7, China patent (2013)
15. Zhou, M., Chu, Z.Y.: Impedance joint torque control of an active-passive composited driving self-adaptive end effector for space manipulator. In: Proceedings of the 11th World Congress on Intelligent Control and Automation, Shenyang, China (2014)
16. Liu, Y.J., Ding, F.: Convergence properties of the least squares estimation algorithm for multivariable systems. Appl. Math. Modell. **37**, 476–483 (2013)